BABEȘ-BOLYAI UNIVERSITY CLUJ-NAPOCA
FACULTY OF BIOLOGY AND GEOLOGY
DOCTORAL SCHOOL OF INTEGRATIVE BIOLOGY

DOCTORAL THESIS

EXPLOITING THE THERAPEUTIC POTENTIAL OF OXIDATIVE STRESS MODULATORS IN MELANOMA

~Summary~

Scientific Supervisor

PROF. DR. ELENA RAKOSY

PhD Candidate

VALENTIN-FLORIAN RAUCA

CLUJ-NAPOCA
2020

BABEȘ-BOLYAI UNIVERSITY CLUJ-NAPOCA
FACULTY OF BIOLOGY AND GEOLOGY
DOCTORAL SCHOOL OF INTEGRATIVE BIOLOGY

DOCTORAL THESIS

EXPLOITING THE THERAPEUTIC POTENTIAL OF OXIDATIVE STRESS MODULATORS IN MELANOMA

~Summary~

Scientific Supervisor

PROF. DR. ELENA RAKOSY

PhD Candidate

VALENTIN-FLORIAN RAUCA

CLUJ-NAPOCA

2020

TABLE OF CONTENTS

LIST OF ABBREVIATIONS

AKT (PKB), protein kinase B; **ANOVA**, Analysis of variance; **ARG-1**, arginase-1; **AUTC**s, Areas under the tumor growth curves; **Bax**, Bcl-2-associated X protein; **Bcl-xL**, B-cell lymphoma-extra-large; **BMDMs**, bone marrow derived macrophages; **CHL**, cholesterol; $CoCl_2$, Cobalt(II) chloride; **DMEM**, Dulbecco's Modified Eagle's Medium; **DMSO**, Dimethyl sulfoxide; **DMXAA**, 5,6-dimethylxanthenone-4- acetic acid; **DPPC**, 1,2-Dipalmitoyl-sn-glycero-3-phosphocholine; **PEG-2000-DSPE**, (N-(Carbonyl-methoxypolyethylene-glycol-2000)-1,2-distearoyl-sn-glycero-3phosphoethanolamine, sodium salt); **dw**, dried weight; **EEAC**, ethanolic extract from aerial parts of *A. chamaepitys*; **EEAG**, ethanolic extract from aerial parts of *A.*

genevensis; **EEAL**, ethanolic extract from aerial parts of *A. laxmannii*; **EMT**, epithelial–mesenchymal transition; **ERK**, extracellular receptor kinase; **FITC**, Fluorescein Isothiocyanate; **GM-CSF**, Granulocyte-macrophage-colony stimulating factor**; GTPase**, guanosine triphosphate hydrolase; **HIF-1α**, hypoxia-inducible factor 1α; **HPLC**, High-Performance Liquid Chromatography; **IC_{50}**, half maximal inhibitory concentration; **IL-12 p40**, Interleukin 12 p40; **IL-12 p70**, Interleukin 12 p70**; IL-13**, Interleukin 13; **IL-1α**, Interleukin 1α; **IL-1β**, Interleukin 1β; **IL-6**, Interleukin 6; **IL-9**, Interleukin 9; **iNOS**, Inducible nitric oxide synthase; **i.v**., Intravenous; **Jun**, proto-oncogene, AP-1 transcription factor subunit; **LCL**, Long circulating liposomes; **M-CSF**, Monocyte-colony stimulating factor; **MDA**, malondialdehyde; **MEK**, MAPK/ERK kinase; **MIG**, Monokine induced by IFN- γ; **MMP-2**, matrix metalloprotease-2; **MMP-9**, matrix metalloprotease-9; **NF-κB**, Nuclear factor κB; **pAP-1-c-Jun**, Phosphorylated form of c-Jun subunit of AP-1; **PI3K**, phosphoinositide 3 kinase; **PLS**, partial least squares regression; **Raf**, rapidly accelerated fibrosarcoma protein; **Ras**, rat sarcoma protein; **RE**, rutin equivalent; **ROS**, reactive oxygen species; **s.c**., Subcutaneous; **SD**, Standard Deviation; **SIM**, Simvastatin; **SNAIL1**, Zinc finger protein SNAI1; **STAT,** signal transducer and activator of transcription; **TAC**, Total antioxidant capacity; **TAMs**, Tumor-associated macrophages; **TGF-β**, transforming growth factor-β; **TIC**, total iridoid content; **TIMP-1**, Tissue inhibitor of metalloproteinase 1; **TIMP-2**, Tissue inhibitor of metalloproteinase 2; **TME**, tumor microenvironment; **TNF-α**, Tumor necrosis factor α; **TPO**, Thrombopoietin; **TPC**, total phenolic content; **VDA**, vascular disrupting agent; **VEGF**, Vascular endothelial growth factor; **VEGFR**, Vascular endothelial growth factor receptor; **Wnt**, Wingless-related integration site; **ZEB1,** Zinc finger E-box-binding homeobox 1.

KEYWORDS: melanoma, oxidative stress modulation, tumor-associated macrophages, combination therapy, simvastatin, 5,6-dimethylxanthenone-4-acetic acid, long-circulating liposomes

Chapter I. Oxidative stress promotes the hallmarks of solid cancers

The more recent integrative approach in cancer treatment highlights the idea of tumor microenvironment, the bed in which multiple distinct cell types are engaged in complex signalling interactions leading to progression and invasion of the disease (Wang et al., 2017). Therefore, tumors are being viewed as organs in relation with the entire organism (Egeblad et al., 2010). The interconnected stromal network consists of tumor cells, tumor associated macrophages (TAMs), dendritic cells, natural killer and natural killer T cells, lymphocytes, tumor associated neutrophils and cancer associated fibroblasts, vascular endothelial cells, myeloid derived suppressor cells, adipocytes, pericytes and other cell types (Balkwill et al., 2012). There are certain factors that contribute to the acquirement of malignant biological capabilities by the tumor microenvironment, acting in a more or less concerted manner. Among these factors, sustained proliferation, induction of apoptosis, invasion and replicative immortality induced by DNA mutations (Hanahan and Weinberg, 2011) are influenced by the oxidative stress status, as described below.

1. Oxidative stress and inflammation, risk factors for melanoma development

An inflammatory microenvironment is known to precede and promote the development of many types of cancer. Excessive UV radiation, as well as prolonged exposure to carcinogenic chemicals can induce persistent inflammation and tumorigenic transformation of skin melanocytes via tumor-initiating DNA mutations (Mantovani et al., 2008). The immune system possesses a vast arsenal of inflammatory response mediators, thus chronic inflammation of the skin can be related either to a hyperactive immune response (allergies) or to auto-inflammation (autoimmune disease) (Dainichi et al., 2014).

On the molecular level, skin cancer is connected to inflammation via distinct intrinsic and extrinsic pathways (Maru et al., 2014). Among intrinsic pathways, the activation of oncogenes, especially from the RAS–RAF–MEK–ERK signalling pathway, is considered a hallmark of malignant melanoma, although other interconnected and simultaneously activated pathways, such as PI3K/AKT, JNK/c-JUN or Wnt/ β-catenin pathway are very common features of this type of cancer (Lopez-Bergami et al., 2008). On the other hand, extrinsic inflammatory pathways are usually triggered by radiation, mechanical, chemical, and biological skin stressors (herpes viruses), which are responsible for chronic inflammation accompanied by oxidative stress

(Khansari et al., 2009). The bridge between the extrinsic and the intrinsic pathways is represented by the activation of inflammation-related transcription factors in pre-cancerous skin cells, mainly NF-κB, HIF-1α and STAT3 with consequent release of inflammatory signalling molecules IL-1, IL-6, IL-8 and TNF-α (Maru et al., 2014). A direct association between the upregulation of pro-inflammatory cytokines and RAS-mediated oncogenic signalling pathway has already been demonstrated in other skin cell types (Cataisson et al., 2012). Free radicals and especially H_2O_2 have inhibitory actions on phosphatases, enzymes that negatively regulate proliferative signalling and kinase networks involved in inflammation. Therefore, free radical levels in tissues can promote inflammatory pathways and aberrant cell proliferation, contributing to cancer development and progression (Meng et al., 2002).

2. Oxidative stress and tumor angiogenesis

Angiogenesis in tumors starts with the so called ‘’angiogenic switch’’, a time-dependent episode in which a shift in the balance between pro- and anti-angiogenic factors occurs, resulting in the onset of *de novo* vessel formation within the tumor stroma (Baeriswyl and Christofori, 2009). Overproduction of VEGF and overexpression of VEGFR are known to play a key role in the formation of such abnormal vascular arborisations, but also in modulating the immune response to tumors and influencing tumor cell signalling via paracrine and autocrine paths (Goel and Mercurio, 2013). The disturbed tumor blood flow induces hypoxic micro-regions which are responsible for the heterogeneity within the same individual tumor, but also for the increased resistance to chemotherapy and radiation therapy (Siemann, 2011). Oxygen restriction leads to adaptive transcriptional responses in affected areas, which are mainly coordinated by HIF family of transcription factors that carry oxygen-responsive α subunits and among them, HIF-1α seems to be a pivotal player (Petrova et al., 2018).

A direct connection between oxidative stress and hypoxia has been established, ROS being responsible for the inactivation of HIF-1α inhibitor prolyl hydroxylase domain (PHD), which leads to HIF-dependent gene expression in favour of angiogenesis (Tafani et al., 2016). There is also a link between inflammation, angiogenesis and oxidative stress reported by research on zebrafish models with high blood vessel resolution in which endothelial cell sprouting, the first step towards neovascularisation, was directly mediated by ROS and NF-κB, without being influenced by hypoxia (Schaafhausen et al., 2013).

3. Oxidative stress enhances the aggressiveness of melanoma cells

The aggressiveness of any type of cancer cell is defined by its ability to develop a resistant and invasive phenotype in favour of quick growth and spreading. The endpoint of this transformation is represented by the colonization of distant organs in a multistep process called metastasis cascade. A pivotal event in melanoma development is the epithelial-mesenchymal transition (EMT), a complex phenotypic transformation of an epithelial cell into a migratory-invasive mesenchymal cell, characterised by overproduction of extracellular matrix (ECM) components that ultimately leads to basement membrane degradation (Kalluri and Weinberg, 2009).

Oxidative stress can affect cell junctions and epithelial barriers by having a stimulatory effect on two of the most important EMT inducing transcription factors ZEB1 and SNAIL1, directly or *via* NF-κB signaling pathway (Imani et al., 2016). The upregulation of transcription factors promoting tumor cell aggressiveness, such as HIF-1α, NF-κB or c-Jun was proved to be in tight connection with the redox status of the cell (Lopez-Bergami et al., 2008). Potential anti-metastatic therapies could destroy tumor circulating cells before extravasation and colonization of distant sites, by inhibiting their ability to counteract the increased oxidative stress they encounter during metastasis (Tasdogan et al., 2020).

4. Oxidative stress and immunosuppression

4.1. The tumor immune microenvironment

Rather than considering them simple masses of aberrantly proliferating cells, modern science describes solid tumors as being abnormal organs composed of tumor cells, immune infiltrate, vascular and lymphatic networks, connective tissue cells, adipocytes other cell populations in tight correlation with the type of cancer and primary tumor location (Balkwill et al., 2012). The tumor immune microenvironment (TIME) is one of the most consistently studied niches within the tumor stroma, because of the potential therapeutic implications of manipulating the immune system for cancer immunotherapy.

Melanoma cells have an arsenal of activated enzymatic and non-enzymatic antioxidant defense systems that protect them against the cumulated oxidative chaos and contribute to the selection of resistant phenotypes (Morry et al., 2017). In addition, most of the immune cells

within the TME (TAMs, TILs, Tregs, MDSCs, neutrophils and eosinophils) can also produce ROS mainly by (NOX-) dependent pathways, increasing the overall oxidative stress to levels which favour suppression of the immune response (Chen et al., 2016). This mutual exchange of catabolites, although beneficial to cancer progression, can also provide perspectives in developing drugs that target the metabolic synergy between tumor cells and other resident stromal cells (Sotgia et al., 2013).

4.2. Macrophage phenotypic plasticity

Mills and his collaborators were the first to observe a fundamental dichotomy in macrophage function, the fact that in response to various growth factors and cytokines ”the big eaters” can differentiate into either inflammatory M1 (Fight) or regulatory M2 (Fix) subtypes which can also promote or inhibit cancer growth (Mills et al., 2000). The M1 phenotype is characterised by high pro-inflammatory IL-12/low immunosuppressive IL-10 cytokine production as opposed to the M2 phenotype which is defined by IL-10 high/IL-12 low cytokine ratio (Mosser and Edwards, 2008). Another major difference between the two subtypes is represented by the way they metabolise the limiting metabolite arginine at sites of inflammation and in tissues with high metabolic demand such as tumors. M1 macrophages express inducible NO synthase (iNOS) enzyme, which uses l-arginine as a substrate to produce large amounts of NO which is a cytotoxic agent as well as an M1 molecular killing arsenal trigger (Ley, 2017). The other enzyme that uses l-arginine as a substrate is the M2 specific arginase which produces significant ammounts of ornithine, a promoter of cell proliferation, tissue repair and angiogenesis (Mills, 2001).

4.3 TAMs promote solid tumor progression and resistance to therapy

TAMs are the most abundant cell population within the TME and most of the infiltrating TAMs are M2 polarized or express an ‘’M2-like phenotype’’, which is responsible for downregulating the activity of other immune cells within the tumor stroma and for promoting tumor growth and cancer cell invasion via cytokines (VEGF, IL-4, IL-10, TGF-β), enzymes (MMPs, Arg-1) and various chemokines (Chen et al., 2019). Therefore, TAMs have a very important pro-tumoral function which helps tumor cells escape immune recognition and supports tumor cell motility.

In melanoma, an abundant macrophage infiltrate is generally associated with poor prognosis because melanoma cells have the ability to produce a high variety of autocrine factors in support of aberrant proliferation, as well as paracrine factors such as IL-10, TGF-β, GM-CSF and CCL2 which can phenotypically turn macrophages into pro-tumor allies. M2-like macrophages ensure the survival of cancer stem cells via arginase derived polyamine synthesis and stimulate the formation of melanoma cell colonies which are thus protected from chemotherapeutic agents (Tham et al., 2014).

Chapter II: ROS modulators as potential game-changers in treating melanoma

1. Reactive oxygen species and antioxidant defence systems

Free radicals are short-lived, unstable and hyper-reactive molecules with odd numbers of electrons, manifesting the tendency to obtain stability by stealing electrons from stable molecules of the living cell (Arulselvan et al., 2016). Previous studies determined that in normal tissues, each cell is exposed to ~1.5×10^5 oxidative hits per day (Perillo et al., 2020). In complex organisms, each tissue holds a specific anti-oxidative potential determined by the amount and activity of non-enzymatic and enzymatic antioxidants within the residing cells, in response to a redox imbalance (Haddad, 2002). The impossibility of the antioxidant systems to compensate a pro-oxidant imbalance eventually leads to oxidative stress. In melanoma, oxidative stress plays a central part in the development, as well as the progression of the disease. High ROS levels can induce adaptive mechanisms in melanoma cells, promoting tumor cell metastatic ability and resistance to therapy (Cannavo et al., 2019).

2. Current therapies in melanoma

2.1. Nanocarriers as drug delivery systems

1) *Liposomes*. Spherical-shaped artificial vesicles, ranging from 5 to 200 nm that have a bilayered structure similar to biological membranes, composed of non-toxic phospholipids and cholesterol**,** extensively used as molecule carriers in pharmaceutical industry because of their ability to trap hydrophobic as well as hydrophilic compounds and release them at designated sites (Akbarzadeh et al., 2013).

2) *Polymer based nanoparticles (NPs)* are natural and synthetic polymers that allow mainly passive, but also active drug targeting.

3. Lipid nanoparticles (LNs) are used as an alternative delivery system to liposomes and NPs due to their higher stability.

4. Other promising nanocarriers used in skin cancer research are represented by exosomes, quantum dots (QD), superparamagnetic iron oxide nanoparticles (SPIONs) and gold nanoparticles (AuNPs).

2.2. Types of targeted therapies in melanoma

The most efficient targeted therapies in this specific type of skin cancer are *oncogenic cascade targeted therapies, cancer immunotherapies* and *anti-angiogenic targeted therapies*.

3. ROS-modulating agents and therapies

3.1. Natural compounds

During the organism's response to stressful conditions, the own antioxidant defence systems can get overwhelmed by the abundance of ROS production and thus exogenous supply of natural antioxidants can have a prophylactic role (Arulselvan et al., 2016). One of the most abundant categories of plant antioxidants is represented by polyphenols, secondary metabolites involved in ultraviolet radiation and pathogen defence, which in food contribute to bitterness, colour, flavour and oxidative stability (Pandey and Rizvi, 2009). There are an outstanding number of studies in favour of the anticancer properties of polyphenols. However, in the light of recent comprehensive meta-analyses on the link between polyphenols and cancer in the last ten years, the most part of the results are of limited clinical significance, being either preliminary or ambiguous and incidental (Grosso et al., 2017).

It is important to make a clear difference between cancer treatment and cancer prevention regarding the use of natural compounds, especially because this aspect is obscure in the majority of *in vitro* studies which seem to ignore the "prevent-impede-delay-cure" as categories of anticancer actions which most of the time do not occur simultaneously (Wang et al., 2012). In addition, phytochemicals display antioxidant activity at low concentrations and pro-oxidant activity at high doses. When taking into account natural compounds as oxidative stress modulators in cancer therapy, the double-edge sword effect of ROS balance, as well as of antioxidant concentration must be taken into account (Valko et al., 2007). Targeted antioxidant therapies can be used to disrupt, maintain or re-establish redox homeostasis, depending on the desired effect in relation to disease type.

3.2. Semi-synthetic compounds: Simvastatin

Besides their primary use as antihypercholesterolemic drugs for coronary heart disease management and prevention, compounds like simvastatin also showed pleiotropic and immunomodulatory effects by regulating oxidative stress, inflammation and endothelial cell

apoptosis (Kirmizis et al., 2010). By inhibiting isoprenoid synthesis, statins can affect the function of isoprenylation-dependent small GTP-binding proteins, Rho, Ras, and Rac which are involved in signalling pathways regulating proliferation, cell motility, cytoskeletal organisation EMT and transcription of various factors that contribute to cancer progression and metastatic phenotypes (Liao and Laufs, 2005; Parri and Chiarugi, 2010).

The anticancer effects of SIM have been described by a consistent number of studies which emphasise different mechanisms of action on different cancer cell lines and tumor models. Before the development of tumor-targeted delivery systems, the relevance of pre-clinical studies on statins remained unclear, due to the fact that less than 5% of a given statin dose actually reached systemic circulation, due of its selective liver localization, which also induced hepatotoxicity and dose-dependent myopathy (Boudreau et al., 2010). Especially in cancer, the tumor-targeting property of liposome-encapsulated SIM can overcome the aforementioned drawbacks (Alupei et al., 2015).

3.3. Synthetic compounds: DMXAA

Vascular disrupting agents (VDAs) represent an attractive anticancer treatment approach because endothelial cells are genetically stable; the tumor endothelium is easily accessible by intravenous therapy and vascular shutdown abruptly and severely deprives the vast majority of tumor cells of vital nutrients and essential gasses (Hinnen and Eskens, 2007). VDAs are oncology agents which have a completely different mechanism of action from that of the classical VEGF/VEGFR-targeted therapies, by taking advantage of the structural and functional differences of the rapidly proliferating tumor endothelium. However, the main drawback of a rapid vascular shutdown consists of a central necrotic area formation in contrast to a viable tumor rim in which aggressive tumor cells with invasive phenotypes are selected (Cooney et al., 2006). This fact and the observation that VDAs tend to interact synergistically with cytotoxic and anti-angiogenic agents encourages their use in combination therapies in which two or more anticancer drugs complement each other's action at lower, more effective doses, targeting the hypoxic tumor core as well as the remaining perfused tumor rim (Siemann and Horsman, 2009; Spear et al., 2011).

DMXAA is a synthetic flavonoid mostly prone to hydrophobic interactions *via* the aromatic 5,6 methyl groups. It was considered a very promising candidate for cancer therapeutics

but it failed human phase III clinical trials due to extreme species sensitivity, being a strong activator of mouse stimulator of interferon genes (mSTING) protein but not human (hSTING), protein, although they have 68% amino acid identity and 81% similarity (Shih et al., 2018). Nevertheless, the process of identifying DMXAA analogues with human activity is on the way (Tijono et al., 2013; Hwang et al., 2019). DMXAA was found to have remarkable antitumor activity in preclinical experiments by selectively arresting blood flow in mouse models of cancer within less than an hour after administration (Baguley, 2003).

3.4. Antioxidant *vs* pro-oxidant therapies.

Antioxidant therapies

Enzymatic as well as non-enzymatic antioxidants are currently viewed as a double-edged sword in cancer treatment. Antioxidant treatments usually have complementary immunomodulatory effects. For example, curcumin is described as a potent modulator of T cells, B cells, macrophages, neutrophils, natural killer cells, and dendritic cells (Jagetia and Aggarwal, 2007) and resveratrol administration as a suppressor of M2-like polarization in lung cancer (Sun et al., 2017). However, the addition of antioxidants at specific doses to lessen chemotherapy-induced oxidative stress has become controversial and there are a lot of factors such as the choice between preventive (low) and therapeutic (high) dose, cancer type or time of observation which need to be taken into consideration before drawing firm conclusions about positive or negative interactions between antioxidants and chemo/radiotherapy (Singh et al., 2018)

Pro-oxidant therapies

A growing body of evidence suggests that antioxidant activities mediated by the leading antioxidant response gene NRF2 counteract the damaging effect of oxidative stress in transformed cells, promoting tumorigenesis and tumor-cell resistance in primary tumors and in CTC, while high levels of NADPH increase the metastatic ability of melanoma (Perillo et al., 2020; Tasdogan et al., 2020). This is in favour of ‘‘Achilles’ heel’’ theory, stating that tumor cell dependence on antioxidants to counteract the higher ROS production compared to normal cells might be their weak point. Therefore, ROS might be considered the “bright side of the moon” in cancer therapy.

Chapter III. The aim of the thesis and general objectives

The aim of this thesis was to develop and evaluate a targeted liposomal therapy with redox modulatory actions in melanoma, a typical representative of ROS driven cancers.

- The **first objective** of of this thesis was to perform a phytochemical screening of several *Ajuga* species used in traditional medicine and to evaluate their anticancer activity on metastatic cell lines susceptible to therapeutic modulation of their redox status.
- The **second objective** of this thesis was to investigate the redox modulatory activity and anticancer potential of a novel combined therapy consisting of SIM and DMXAA on an *in vitro* model of melanoma microenvironment
- **The third objective** of this thesis was to assess the oxidative stress modulating potential and anti-melanoma efficacy of the novel combined therapy consisting of LCL-SIM and LCL-DMXAA on an *in vivo* murine melanoma model

Chapter IV. Biologically Active Ajuga Species Extracts Modulate Supportive Processes for Cancer Cell Development

This chapter was published as Valentin-Florian Rauca, Laurian Vlase, Tibor Casian, Alina Sesarman, Ana-Maria Gheldiu, Andrei Mocan, Manuela Banciu, Anca Toiu, Biologically active ajuga species extracts modulate supportive processes for cancer cell development, Frontiers in Pharmacology, 2019; 10:334, doi: 10.3389/fphar.2019.00334

1. Introduction

Ajuga species have been used in traditional medicine for their diuretic, anti-inflammatory, wound-healing, and hepatoprotective properties. The phytochemical profile and anticancer potential of three *Ajuga* sp. (*A. genevensis*, *A. chamaepitys*, and *A. laxmannii*) from Romania was investigated. *Ajuga laxmannii* ethanol extract showed the highest total phenolic and flavonoid content, while *A. genevensis* ethanol extract was more abundant in iridoids. The overall cytostatic effect of the investigated plant extracts was exerted through strong inhibitory actions on NF-κB, the key molecule involved in the inflammatory response and via oxidative stress modulatory effects in both murine colon carcinoma and melanoma cell lines. *Ajuga laxmannii* showed the most significant antitumor activity and represents an important source of

bioactive compounds, possibly an additional form of treatment alongside conventional anticancer drugs.

2. Materials and Methods

The phytochemicals were extracted from the aerial parts of *Ajuga* sp. by using different solvents and methods. The hydroalcoholic extracts were examined for total phenolic, flavonoid and iridoid contents, and HPLC/MS was used to analyze the polyphenolic compounds and iridoids. The phytochemical profile was also evaluated by principal component analysis in connection with antitumor efficacy of extracts. The antiproliferative potential was evaluated using the ELISA BrdU-colorimetric immunoassay. Western Blot with regard to inflammatory protein NF-κB (nuclear factor kappa-light-chain-enhancer of activated B cells) p65 subunit expression in cell lysates was performed. Quantification of oxidative stress marker malondialdehyde (MDA) was determined by high-performance liquid chromatography (HPLC). Enzymatic and non-enzymatic antioxidant capability was assessed by measuring catalase activity and by evaluating the total antioxidant capacity (TAC) of treated cells.

3. Results and discussion

3.1. Antiproliferative activity of *Ajuga sp*. extracts on C26 and B16.F10 cancer cell lines

The effects of different treatments at various concentrations (50–650 µg /mL) on the proliferation of C26 and B16.F10 cells were expressed as percentage of inhibition compared to the proliferation of the untreated control cells (**Figures 1 A,B**) and as IC_{50} values for each extract tested (**Table 1**).

Our data showed that EEAL exerted strong inhibitory effects at much lower concentrations than EEAC and EEAG on B16.F10 melanoma (**Figure 1A** and **Table 1**) as well as on C26 Colon Carcinoma Cells (**Figure 1B** and **Table 1**). The relationship between input variables (plant species, extract concentration, cell type – X dataset) and cell proliferation inhibition rate (Y dataset) was assessed by fitting a polynomial equation through PLS method. The specific types of polyphenols (isoquercitrin, rutin and apigenin) and iridoids (harpagoside and 8-*O*-acetyl-harpagide) might be involved in strong antitumor activity of the plant extracts tested.

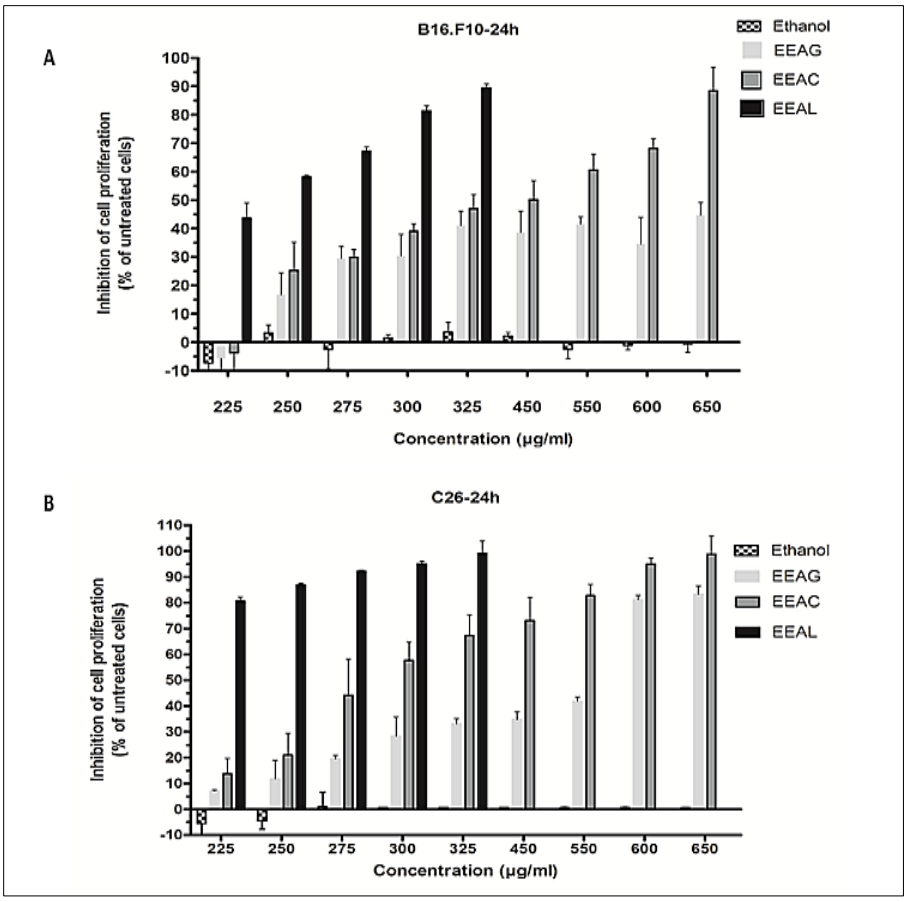

Figure 1: Effects of *Ajuga* sp. extracts on cell proliferation. (A) 24 h after incubation of B16.F10 cells with different concentrations of EEAG, EEAC, and EEAL extracts. **(B)** 24h after incubation of C26 cells with different concentrations of EEAG, EEAC, and EEAL extracts. Data are shown as mean ± SD of triplicate measurements. EEAG, *A. genevensis* ethanolic extract; EEAC, *A. chamaepitys* ethanolic extract; EEAL, *A. laxmannii* ethanolic extract. Ethanol-treated cells were used as toxicity controls.

Table 1: Cytotoxicity of *Ajuga* sp. ethanolic extracts against C26 and B16.F10 murine cancer cell lines by ELISA BrdU-colorimetric immunoassay (IC_{50} value, µg/mL).

Cell line	**C26**		**B16.F10**	
Treatment	**IC_{50}**	**Confidence interval 95%**	**IC_{50}**	**Confidence interval 95%**
EEAG (*A. genevensis*)	457.5	374.0 to 559.7	741.4	388.5 to 1415
EEAC (*A. chamaepitys*)	303.0	274.8 to 334.1	406.7	341.7 to 484.1
EEAL (*A. laxmannii)*	176.3	154.5 to 201.1	236.8	227.1 to 246.8

IC_{50} represents the half maximal inhibitory concentration for the tested drugs.

3.2. Strong inhibitory actions of the vegetal extracts on NF-κB-p65 expression in C26 and B16.F10 total cell lysates

Our results indicated that IC_{80} concentrations of all *Ajuga* sp. extracts tested in this study (IC_{40} in the case of EEAG tested on B16.F10) elicited a very strong inhibition (≥ 80% compared with control) of the key inflammatory transcription factor NF-κB-p65 expression (**Figures 2 A-D**).

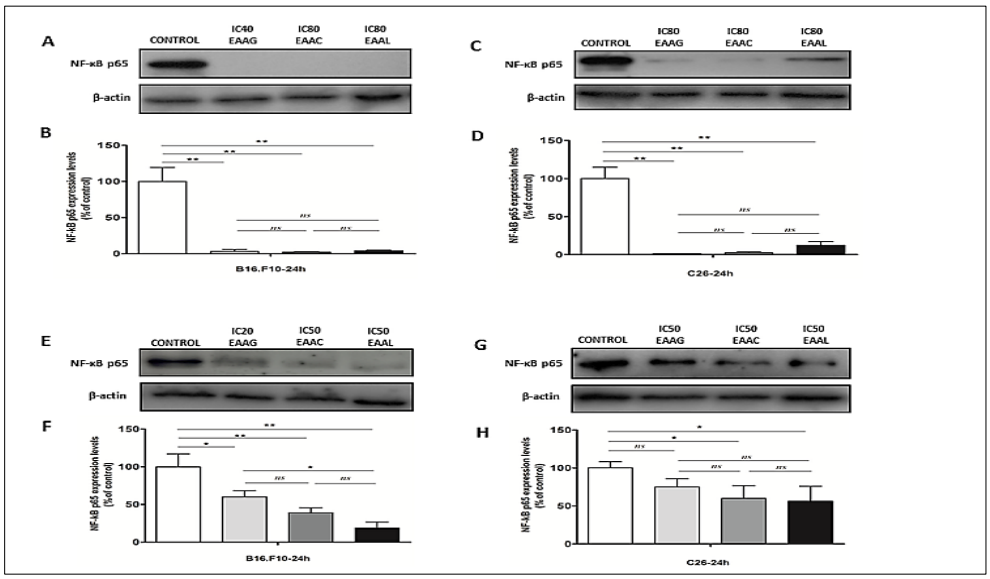

Figure 2: The expression of NF-κB-p65 in cell lysates after different treatments. Western blot analysis of total NF-κB-p65 expression in cell lysates from (**A,E**) B16.F10 cells and (**C,G**) C26 cells after different treatments; b-actin was used as loading control. (**B**) % of NF-κB-p65 expression relative to control in B16.F10 melanoma cells after IC_{40} EEAG, IC_{80} EEAC, and IC_{80} EEAL treatments. (**F**) % of NF-κB-p65 expression relative to control in B16.F10 melanoma cells after IC_{20} EEAG, IC_{50} EEAC, and IC_{50} EEAL treatments. (**D**) % of NF-κB expression relative to control in C26 colon carcinoma cells after IC_{80} EEAG, IC_{80} EEAC, and IC_{80} EEAL treatments. (**H**) % of NF-κB expression relative to control in C26 colon carcinoma cells after IC_{50} EEAG, IC_{50} EEAC, and IC_{50} EEAL treatments. On B16.F10 cells: Control, untreated cells; IC_{40} or IC_{20} EEAG, cells incubated with 650 μg/mL or 260 μg/mL *A. genevensis* ethanolic extract; IC_{80} or IC_{50} EEAC, cells incubated with 650 μg/mL or 406.7μg/mL *A. chamaepitys* ethanolic extract; IC_{80} or IC_{50} EEAL, cells incubated with 325 μg/mL or 236.8 μg/mL *A. laxmannii* ethanolic extract. On C26 cells: Control, untreated cells; IC_{80} or IC_{50} EEAG, cells incubated with 650 μg/mL or 457.5 μg/mL *A. genevensis* ethanolic extract; IC_{80} or IC_{50} EEAC, cells incubated with 650 μg/mL or 303 μg/mL *A. chamaepitys* ethanolic extract; IC_{80} or IC_{50} EEAL, cells incubated with 325 μg/mL or 176.3 μg/mL *A. laxmannii* ethanolic extract. Results represent the mean ± SD of two independent measurements. One way ANOVA test with Bonferroni correction for multiple comparisons was used to analyze the effects of different treatments on the levels of NF-κB-p65 in comparison with the pro-inflammatory transcription factor production in control (ns, $P > 0.05$; *$P < 0.05$;**$P < 0.01$).

In addition, the IC_{50} concentrations (**Table 1**) tested on both cell lines (IC_{20} in the case of EEAG tested on B16.F10) determined various levels of inhibition (30–70% compared with control) (**Figures 2 E–H**).

3.3. Modulatory effects of Ajuga sp. extracts on "physiological" oxidative stress of cancer cells

As cancer cells are under persistent oxidative stress (Alupei et al., 2015), we investigated the potential relationship between the antiproliferative activity of the vegetal extracts, and oxidative stress generated in both cancer cell types. Thus, the levels of a general oxidative stress marker – MDA, as well as the catalytic activity of catalase and production of non-enzymatic antioxidant systems were assessed on both cell lines and are shown in **Figure3, 4**.

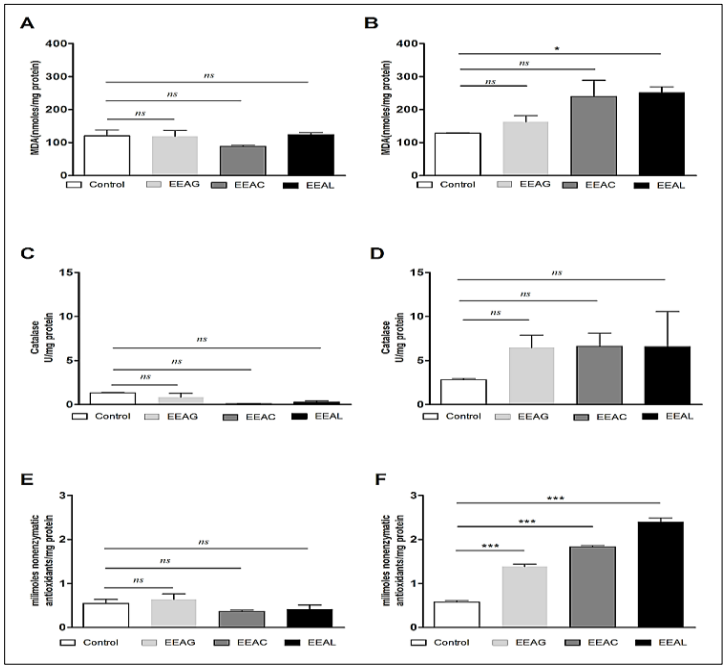

Figure 3: Effects of *Ajuga* sp. extracts on the oxidative stress generated by C26 colon carcinoma cells. (**A, B**) Malondialdehyde (MDA) concentration after (**A**): IC_{50} EEAG, IC_{50} EEAC, IC_{50} EEAL treatment and (**B**): IC_{80} EEAG, IC_{80} EEAC, IC_{80} EEAL treatment. (**C, D**) Catalytic activity of catalase after (**C**): IC_{50} EEAG, IC_{50} EEAC, IC_{50} EEAL treatment, and (**D**): IC_{80} EEAG, IC_{80} EEAC, IC_{80} EEAL treatment. and (**E, F**) Total nonenzymatic antioxidant system levels in the cell lysates obtained from standard culture of C26 colon carcinoma cells after 24h of incubation with (**E**): IC_{50} EEAG, IC_{50} EEAC, IC_{50} EEAL treatment, and (**F**): IC_{80} EEAG, IC_{80} EEAC, IC_{80} EEAL treatment. One way ANOVA test with Bonferroni correction for multiple comparisons was performed to analyze the differences between the effects of the treatments applied on MDA and nonenzymatic antioxidant defense systems levels and on catalase activity. Control= untreated C26 cells; IC_{80} or IC_{50} EEAG: cells incubated with 650 µg/mL or 457.5 µg/mL *A. genevensis* ethanolic extract; IC_{80} or IC_{50} EEAC: cells incubated with 650 µg/mL or 303 µg/mL *A. chamaepitys* ethanolic extract; ; IC_{80} or IC_{50} EEAL: cells incubated with 325 µg/mL or 176.3 µg/mL *A. laxmannii* ethanolic extract. (*ns*, $P>0.05$; *, $P<0.05$; ***, $P<0.001$).

Our results indicated that the IC_{80} concentrations of the extracts (IC_{40} in the case of EEAG on B16.F10) increased the pro-oxidative damage (**Figures 3B**, **4B**) in correlation with a proportional increase in the antioxidant capacity of the remaining cancer cells (**Figures 3F**, **4F**)

of both cell lines. The activity of the antioxidant enzyme catalase on both cell lines was not significantly modified by the IC_{80} extract concentrations used in this investigation (**Figures 3D**, **4D**).

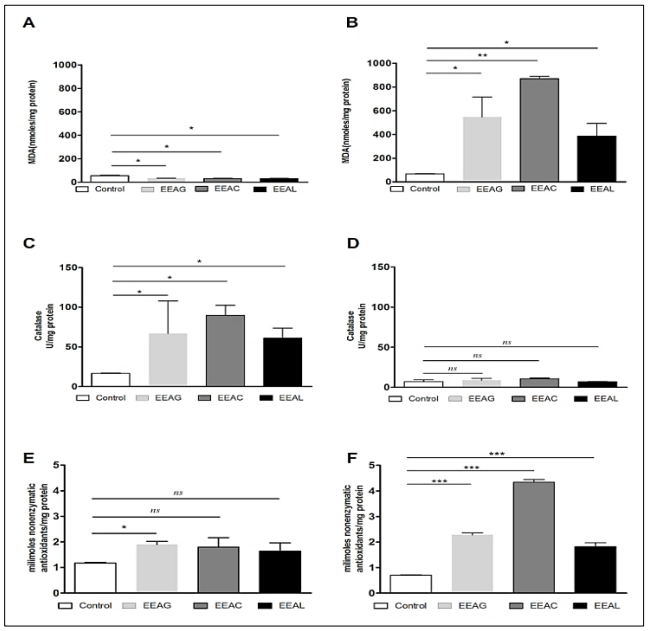

Figure 4: Effects of *Ajuga* sp. extracts on the oxidative stress generated by B16.F10 melanoma cells. (**A, B**) Malondialdehyde (MDA) concentration after (**A**): IC_{20} EEAG, IC_{50} EEAC and IC_{50} EEAL treatment and (**B**): IC_{40} EEAG, IC_{80} EEAC and IC_{80} EEAL treatment. (**C, D**) Catalytic activity of catalase after (**C**) IC_{20} EEAG, IC_{50} EEAC and IC_{50} EEAL treatment and (**D**): IC_{40} EEAG, IC_{80} EEAC and IC_{80} EEAL treatment. (**E, F**) Total nonenzymatic antioxidant system levels in the cell lysates obtained from standard culture of B16.F10 murine melanoma cells after 24h of incubation with (**E**): IC_{20} EEAG, IC_{50} EEAC and IC_{50} EEAL treatment and (**F**): IC_{40} EEAG, IC_{80} EEAC and IC_{80} EEAL treatment.. One way ANOVA test with Bonferroni correction for multiple comparisons was performed to analyze the differences between the effects of the treatments applied on MDA and nonenzymatic antioxidant defense systems levels and on catalase activity. Control= untreated B16.F10 cells; IC_{40} or IC_{20} EEAG: cells incubated with 650 µg/mL or 260 µg/mL *A. genevensis* ethanolic extract; IC_{80} or IC_{50} EEAC: cells incubated with 650 µg/mL or 406.7 µg/mL *A. chamaepitys* ethanolic extract; IC_{80} or IC_{50} EEAL: cells incubated with 325 µg/mL or 236.8 µg/mL *A. laxmannii* ethanolic extract. (*ns*, $P>0.05$; *, $P<0.05$; **, $P<0.01$; ***, $P<0.001$).

However, the IC_{50} extract concentrations (IC_{20} in the case of EEAG) had a moderate antioxidant effect on B16.F10 cells by reducing the levels of MDA compared to control (**Figure 4A**) and slightly stimulating catalase activity (**Figure 4C**). On C26 cells, the IC_{50} extract concentrations did not significantly modify any of the parameters of oxidative stress tested (**Figures 3 A, C, E**).

4. Conclusion

In conclusion, the results of our study indicated that the overall cytostatic effect of the investigated plant extracts was exerted through strong inhibitory actions on NF-κB-p65, the key

molecule involved in the inflammatory response, and *via* oxidative stress modulatory effects in both murine colon carcinoma and melanoma cell lines. Among the three selected species, *Ajuga laxmannii* elicited the strongest inhibitory action at lower doses on B16.F10 and C26 cancer cell lines, compared to *Ajuga chamaepitys* and *A. genevensis*, due to the its richer composition in bioactive polyphenolic compounds. Nevertheless, extended studies on experimental tumor models could shed more light on the anticancer activity of the selected indigenous *Ajuga* sp. extracts. Our results indicated that *Ajuga laxmannii* extract holds the potential to become an additional form of treatment alongside conventional anticancer drugs.

Chapter V. Combination therapy of simvastatin and 5, 6-dimethylxanthenone-4-acetic acid synergistically suppresses the aggressiveness of B16.F10 melanoma cells

This chapter was published as Valentin-Florian Rauca, Emilia Licarete, Lavinia Luput, Alina Sesarman, Laura Patras, Paul Bulzu, Elena Rakosy-Tican, Manuela Banciu, Combination therapy of simvastatin and 5, 6-dimethylxanthenone-4-acetic acid synergistically suppresses the aggressiveness of B16.F10 melanoma cells, PLoS ONE, 2018; 23;13(8):e0202827, doi: 10.1371/journal.pone.0202827

1. Introduction

The major drawback of current anti-angiogenic therapies is drug resistance, mainly caused by overexpression of the transcription factor, hypoxia-inducible factor 1α (HIF-1α) as a result of treatment-induced hypoxia, which stimulates cancer cells to develop aggressive and immunosuppressive phenotypes. Moreover, the cancer cell resistance to anti-angiogenic therapies is deeply mediated by the communication between tumor cells and tumor-associated macrophages (TAMs)-the most important microenvironmental cells for the coordination of all supportive processes in tumor development. Thus, simultaneous targeting of TAMs and cancer cells could improve the outcome of the anti-angiogenic therapies. Since our previous studies proved that simvastatin (SIM) exerts strong antiproliferative actions on B16.F10 murine melanoma cells via reduction of TAMs-mediated oxidative stress and inhibition of intratumor production of HIF-1α, we investigated whether the antitumor efficacy of the anti-angiogenic agent-5,6-dimethylxanthenone-4-acetic acid (DMXAA) could be improved by its co-administration with the lipophilic statin. Our results provide confirmatory evidence for the ability of the combined treatment to suppress the aggressive phenotype of the B16.F10 melanoma cells

co-cultured with TAMs under hypoxia-mimicking conditions in vitro. Thus, proliferation and migration capacity of the melanoma cells were strongly decelerated after the co-administration of SIM and DMXAA. Moreover, our data suggested that the anti-oxidant action of the combined treatment, as a result of melanogenesis stimulation, might be the principal cause for the simultaneous suppression of key molecules involved in melanoma cell aggressiveness, present in melanoma cells (HIF-1α) as well as in TAMs (arginase-1). Finally, the concomitant suppression of these proteins might have contributed to a very strong inhibition of the angiogenic capacity of the cell co-culture microenvironment.

2. Materials and methods

B16.F10 murine melanoma cells (ATCC, CRL-6475) were cultured in Dulbecco's Modified Eagle's medium (DMEM, Lonza, Basel, CH), supplemented with 10% heat-inactivated fetal bovine serum, 100 IU/ml penicillin, 100 μg/ml streptomycin and 4mM L-glutamine as monolayer at 37° C in a 5% CO_2 humidified atmosphere. After differentiation of bone marrow cells into BMDMs, these cells were harvested (Zhang et al., 2008) and co-cultured with B16.F10 cells at a cell density ratio of 4:1 that approximates the physiological conditions of murine melanoma development *in vivo* (Haase-Kohn et al., 2014; Luput et al., 2017). To mimic hypoxic intratumor levels of HIF-1α, cells were incubated for 24h with culture medium supplemented with 200 μM cobalt(II) chloride ($CoCl_2$) – an established inducer of HIF-1α stabilization (Al Okail, 2010). DMXAA (Selleckchem, Houston, TX, USA) was prepared in 100 % dimethyl sulfoxide (DMSO) and kept frozen at –20 °C. SIM (Sigma-Aldrich, MO, USA) was dissolved in ethanol 70% to prepare stock solutions. To determine the effects of different treatments on B16.F10 murine melanoma cells proliferation, 1×103 cancer cells/well were co-cultured with macrophages as shown above, in 96-well plates for 24 h. The proliferative activity of the cancer cells after different treatments was tested using ELISA BrdU-colorimetric immunoassay (Roche Applied Science, Penzberg, DE). To determine whether inhibition of cell proliferation is due to the induction of apoptosis in the co-culture of B16.F10 melanoma cells and macrophages under hypoxic conditions, Annexin V-fluorescein isothiocyanate (FITC) assay (Cayman Chemical, Ann Arbor, MI, USA) was used. To determine the cell migration capacity, B16.F10 murine melanoma cells co-cultured with macrophages at a cell density ratio of 1:4 were seeded in 24-well plates. After 24 h, the confluent cell monolayers were wounded by a plastic tip (1 mm) as

shown previously (Liang et al., 2007). Cells were monitored under a microscope equipped with photo camera at time 0 (time of scratching) and at 24 h after scratching.

For the molecular analysis, cell lysates were prepared. Quantification of malondialdehyde (MDA) by HPLC analysis, determination of melanin content, western blot analysis of HIF- 1α levels, angiogenic protein array (RayBio® Mouse Angiogenic protein Antibody Array membranes 1.1, RayBiotech Inc., Norcross, GA, USA) and RT- qPCR quantification of TAMs markers expression and nitric oxide metabolites production in TAMs were performed. Data from different experiments were indicated as mean ± standard deviation (SD).

3. Results and discussion

3.1. Synergistic action of SIM and DMXAA on murine melanoma cell proliferation

The effects of different treatments on the proliferation of B16.F10 cells in monoculture and in the presence of TAMs under hypoxia-mimicking conditions were expressed as percentage of inhibition compared to the proliferation of the untreated cells (control cells) (**Figure 5 A-C**) and as IC_{50} values for each drug tested (Hiss et al., 2007) presented in **Table 2**.

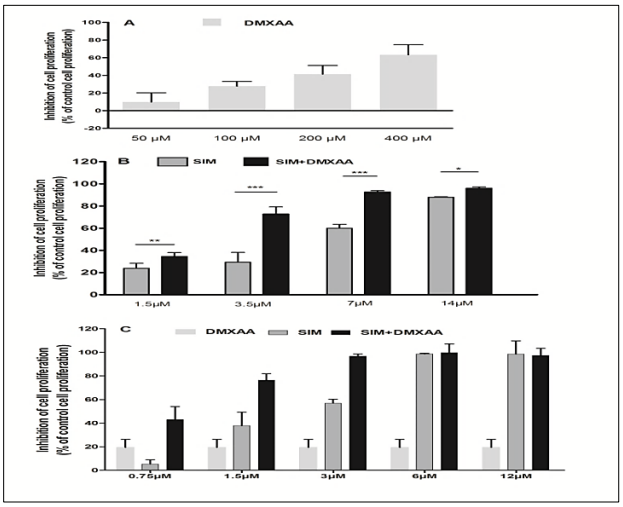

Figure 5: Effects of the combined administration of SIM and DMXAA on B16.F10 cell proliferation under hypoxia-mimicking conditions. (A) 24 h after incubation of co-culture of B16.F10 cells and TAMs with different concentrations of DMXAA; **(B)** 24 h after incubation of co-culture of B16.F10 cells and TAMs with different concentrations of SIM administered alone or in combination with 100 μM DMXAA; **(C)** 24 h after incubation of mono-cultured B16.F10 cells with 100 μM DMXAA administered alone and with different concentrations of SIM administered alone or in combination with 100 μM DMXAA. Data are shown as mean ± SD of triplicate measurements; DMXAA: cells incubated with different concentrations of DMXAA; SIM: cells incubated with

different concentrations of SIM; SIM+ 100 μM DMXAA: cells incubated with different concentrations of SIM administered in combination with 100 μM DMXAA; The two-way ANOVA Multiple Comparison Test with Bonferroni post-tests was used to compare overall effects of different drug concentrations (*, $P<0.05$; **, $P<0.01$; ***, $P<0.001$).

Table 2: Synergistic effect of the co-administered SIM and DMXAA on B16.F10 cells proliferation in the presence of TAMs.

Treatment	IC_{50}	Confidence interval 95%	Combination index (CI)	
			CI value	Interpretation
SIM	4.825	1.232 to18.89	-	-
DMXAA	288.1	209.2 to 396.9	-	-
SIM+100 μM DMXAA	2.088	1.933 to 2.256	0.77	Synergism

IC_{50} represents the half maximal inhibitory concentration for the tested drugs and **CI** represents the "combination index", which quantitatively depicts synergism (CI < 1), additive effect (CI = 1), and antagonism (CI > 1), according to Chou-Talalay method.

Since the 100 μM DMXAA was the first concentration that inhibited moderately B16.F10 cell proliferation in co-culture (by 30% compared to the proliferation of control cells) (**Figure 5A**), this concentration was selected for combination treatments with different concentrations of SIM (**Figure 5B**). Notably, the association of 100 μM DMXAA with every SIM concentration tested enhanced statistically significantly the antiproliferative effects of SIM on monocultured, as well as co-cultured tumor cells (**Figure 5 B-C**). Moreover, the IC_{50} of SIM decreased 1.8 times when the statin treatments were administered in combination with 100 μM DMXAA on the co-cultured cells (**Table 2**).

3.2 The migration capacity of B16.F10 melanoma cells was affected by the combined treatment

To assess whether the applied treatment affected the invasive capacity of B16.F10 murine melanoma cells co-cultured with TAMs, we performed the monolayer cell migration assay (**Figure 6A**). Our results suggested that all treatments applied inhibited strongly tumor cell migration. Nevertheless, the suppressive effect exerted by the combined treatment was higher than those exerted by each single drug treatment (**Figure 6A-B**). Thus, the combined administration of SIM and DMXAA inhibited almost completely the migration of B16.F10 cells (more than 90% inhibition compared to the migration of untreated cells), while the administration of either DMXAA or SIM suppressed by 50-75% the invasive capacity of these

cancer cells (**Figure 6B**). This finding suggested that the aggressive phenotype of B16.F10 cells might be affected by the tested treatments.

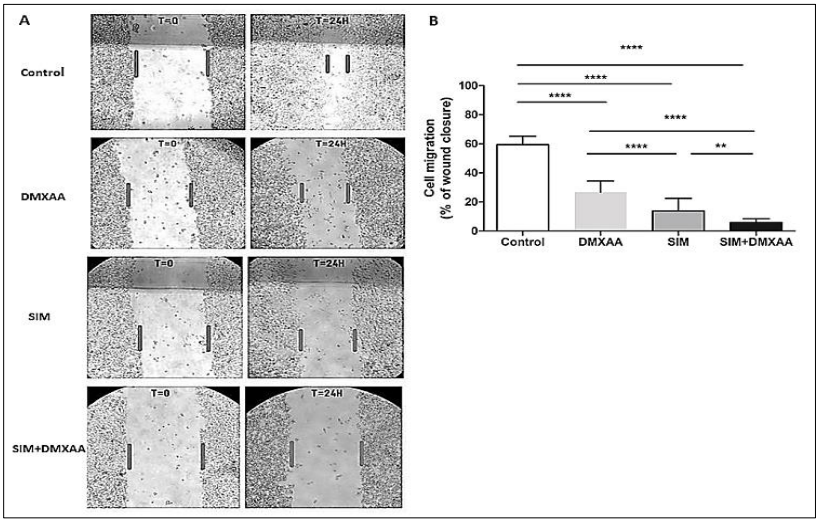

Figure 6: **Assessment of the migration capacity of B16.F10 melanoma cells co-cultured with TAMs after different treatments. (A)** B16.F10 cells co-cultured with TAMs before administration (T=0) and 24 h after administration (T=24H) of different treatments. Four images per well were taken for each condition (Fig 3A, magnification 100*x*). **(B)** The cell migration quantification. The cell migration was estimated by percentages of wound closure compared to the width of the wound at T=0. Control= untreated cells in co-culture; DMXAA: cell co-culture incubated with 100 µM DMXAA; SIM: cell co-culture incubated with 3.5 µM SIM, SIM+DMXAA: cell co-culture incubated with 3.5 µM SIM administered in combination with 100 µM DMXAA. One-way ANOVA with Bonferroni correction for multiple comparisons was performed to determine the statistical significance (**, $P<0.01$; ****, $P<0.0001$).

3.3. Strong anti-oxidant effects of SIM and DMXAA on B16.F10 co-cultured with TAMs

To link the effects of the treatments on the cancer cell proliferation and migration to the modulation of the oxidative stress (Luput et al., 2017) in the co-culture model, we determined the levels of MDA- the lipid peroxidation product, a general marker for oxidative stress (Patras et al., 2016). Our results showed that oxidative stress was notably suppressed by all treatments, but the strongest inhibition was caused by the combined treatment, which almost completely reduced the MDA levels in cell co-culture lysates (higher than 90% reduction compared to the production of MDA in control cells) (**Figure 7**). These data suggested that the very strong anti-oxidant action of the combined therapy might be responsible for the inhibition of migration capacity of these cells, but also for the suppression of B16.F10 cell proliferation presented above.

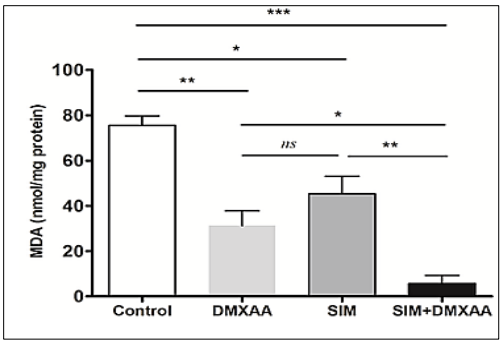

Figure 7: The effects of different treatments on the MDA levels from the co-culture of B16.F10 cells and TAMs, incubated under hypoxia-mimicking conditions for 24 h. The results are expressed as mean ± SD of two independent measurements. Control= untreated cells in co-culture; DMXAA: cell co-culture incubated with 100 μM DMXAA; SIM: cell co-culture incubated with 3.5 μM SIM, SIM+DMXAA: cell co-culture incubated with 3.5 μM SIM administered in combination with 100 μM DMXAA. One way ANOVA test with Bonferroni correction for multiple comparisons was performed to analyze the differences between the effects of the treatments applied on MDA levels (*ns*, $P>0.05$; *, $P<0.05$; **, $P<0.01$; ***, $P<0.001$).

3.4. The effects of the combined treatment on the melanin content in the cell co-culture

As melanin content modulates melanoma oxidative stress (Denat et al., 2014) and the aggressive phenotype of cancer cells, the effects of the treatments on this specific pigment production in the co-culture model were assessed. Our results showed that only the combined treatment elicited the melanin production in B16.F10 melanoma cells (**Figure 8**).

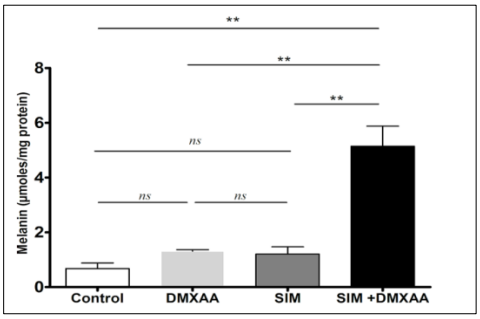

Figure 8: The effects of different treatments on the melanin content in the cell co-culture. The results are expressed as mean ± SD of two independent measurements. Control= untreated cells in co-culture; DMXAA: cell co-culture incubated with 100 μM DMXAA; SIM: cell co-culture incubated with 3.5 μM SIM, SIM+DMXAA: cell co-culture incubated with 3.5 μM SIM administered in combination with 100 μM DMXAA. One way ANOVA test with Bonferroni correction for multiple comparisons was performed to analyze the differences between the effects of the treatments applied on melanin content (*ns*, $P>0.05$; **, $P<0.01$).

Thus, the cell co-culture incubated simultaneously with SIM and DMXAA presented a 7.5-fold higher level of melanin than in control cell co-culture ($P<0.01$).

3.5. The angiogenic capacity of cell co-culture microenvironment was strongly inhibited by the combined treatment

To assess the effects of treatments on angiogenic capacity of the co-culture microenvironment under hypoxia-mimicking conditions, a screening for 24 angiogenic/inflammatory proteins was performed using protein array and the results are shown in **Figure 9**.

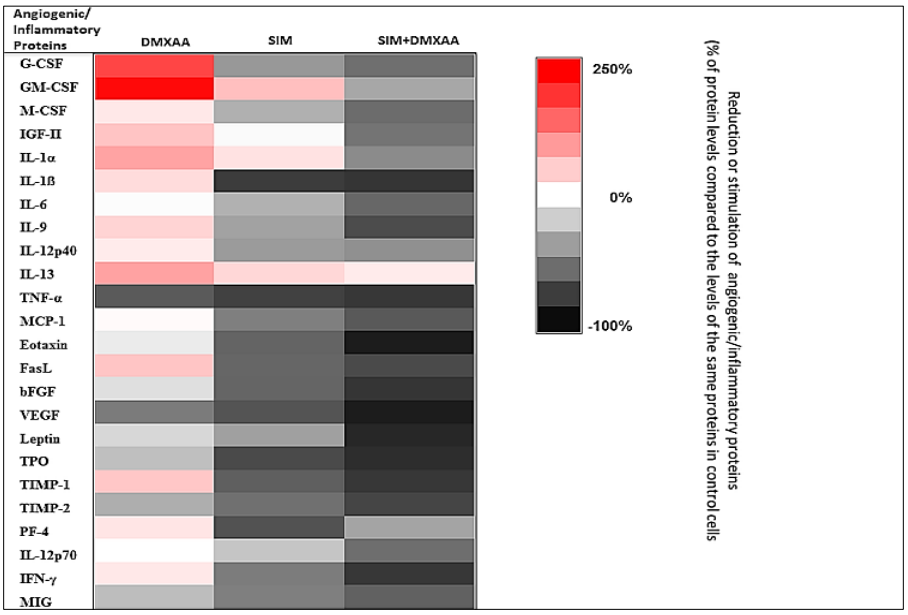

Figure 9: **The effects of different treatments on angiogenic and inflammatory proteins production in the co-culture of B16.F10 melanoma cells and TAMs.** The protein levels after different treatments are compared with the levels of the same proteins in control cells. Data are expressed as average % of reduction (-) of protein levels ranging from 0% (white) to -100% (black) or stimulation (+) of production of proteins ranging from 0% (white) to +250% (red) compared with the levels of the same proteins in control cells. DMXAA: cells incubated with 100 µM DMXAA; SIM: cells incubated with 3.5 µM SIM, SIM+DMXAA: cells incubated with 3.5 µM SIM administered in combination with 100 µM DMXAA.

3.6. The combined treatment partially "re-educated" TAMs

To investigate whether the suppressive effects on main pro-tumor processes coordinated by TAMs could be linked to the "re-education" capacity of the combined treatment, the expression of specific markers for M2 (ARG-1 and IL-10) (Sica et al., 2006), as well as M1 phenotype (the level of nitrite – the final product of the metabolism of nitric oxide resulted from inducible nitric oxide synthase (iNOS) activity (Mills et al., 2000)) were assessed. Our data showed that only the expression level of ARG-1 was strongly reduced by 80% after TAMs incubation with the combined treatment (**Figure 10 A-B**).

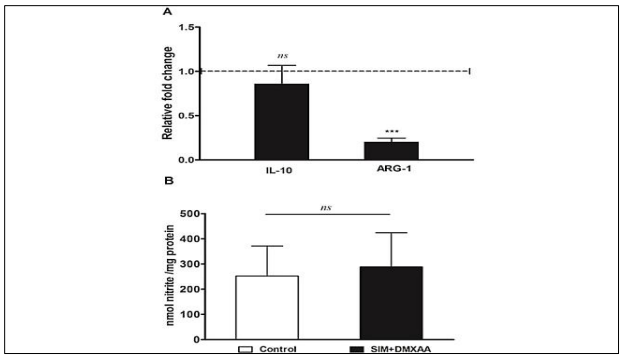

Figure 10: The effects of the combined treatment on macrophage polarization. (A) Effects of SIM and DMXAA co-administration on the levels of ARG-1 and IL-10 mRNA in IL-4-treated BMDMs under hypoxia-mimicking conditions. mRNA was quantified by RT-qPCR and the results are expressed as fold change based on the Ct calculations. Untreated cells were used as calibrator. The results are expressed as mean ± SD of three independent measurements **(B)** Nitrite levels in lysates from IL-4-treated BMDMs incubated with SIM co-administered with DMXAA under hypoxia-mimicking conditions. The results are expressed as mean ± SD of two independent measurements. Control = untreated IL-4 polarized macrophages; SIM+DMXAA = IL-4 polarized macrophages treated with 3.5 μM SIM and 100 μM DMXAA (*ns*, $P>0.05$; ***, $P<0.001$).

4. Conclusion

In conclusion, our data demonstrated that the combined administration of SIM and DMXAA on the co-culture of B16.F10 murine melanoma cells and TAMs under hypoxia-mimicking conditions has the potential to become a successful targeted microenvironment therapy, based on the strong anti-oxidant action on the co-culture milieu and suppression of cancer cell aggressive phenotype.

Chapter VI. Co-administration of liposome-encapsulated agents simvastatin and DMXAA disrupts key molecular mechanisms of malignant melanoma progression

This chapter is a manuscript in preparation for submission as: Valentin-Florian Rauca, Laura Pătraș, Lavinia Lupuț, Emilia Licărete, Vlad Toma, Alina Porfire, Augustin C. Moț, Alina Sesărman, Elena Rakosy-Tican, Manuela Banciu. Co-administration of liposome-encapsulated agents simvastatin and DMXAA disrupts key molecular mechanisms of malignant melanoma progression.

1. Introduction

The aberrant activation of multiple interconnected signaling pathways poses a big challenge that scientists trying to pinpoint the specific mechanisms of melanoma progress and

development need to overcome. On the other hand, as an exponent of reconfigured signaling pathways, melanoma is an attractive option for targeted drug development. The major setback in the use of vascular disrupting agents (VDAs) against solid tumors like melanoma is represented by peripheral tumor resistance in hypoxic zones characterized by hypoxia-inducible factor 1α (HIF-1α) overexpression. Therefore, combining a potent VDA with an anti-angiogenic/cytotoxic agent might overcome current tumor resistance issues The ability of co-administered simvastatin and 5, 6-dimethylxanthenone-4-acetic acid (DMXAA) to suppress the aggressive phenotype of B16.F10 melanoma cells co-cultured with tumor associated macrophages under hypoxia-mimicking conditions was already demonstrated *in vitro* studies. Thus, the aim of the present study was to evaluate the effectiveness of the two therapeutic agents incorporated in polyethylene glycol-coated long circulating liposomes (LCL) on an *in vivo* murine melanoma model. Our results indicated that effective inhibition of murine melanoma growth by the combined liposomal therapy was based on inducing an anti-angiogenic and pro-apoptotic state of the tumor microenvironment and maintained via suppression of major invasion and metastasis promoters. In conclusion, this novel targeted approach might overcome the aggressive transformations mediated by the emergence of marginal hypoxic tumor sites post-VDA administration.

2. Materials and methods

The molar ratio of compounds used for LCL-SIM preparation was 17:1.01:1:1.209 (DPPC:PEG-2000-DSPE:CHL:SIM). The molar ratio of compounds used for the preparation of the novel DMXAA liposomal formulation was 1.85:0.7:0.3:0.15 (DPPC:CHL:DMXAA:PEG-2000-DSPE).

B16.F10 murine melanoma cells (ATCC, CRL-6475) were cultured in DMEM according to our previous studies. Syngeneic male C57BL/6 mice 6 to 8-week-old (Cantacuzino Institute, Bucharest, RO) kept under standard laboratory conditions were inoculated with 1×10^6 B16.F10 cells *s.c.* in the right flank. Each experimental group contained 5-6 mice.

The effects of liposome-encapsulated agents SIM and DMXAA on tumor growth were compared to the effects of free active agents on B16.F10 murine melanoma-bearing mice. LCL-

SIM (5 mg/kg) and LCL-DMXAA (14 mg/kg) were simultaneously as well as separately administered in the caudal vein, on days 11 and 14 after tumor cell inoculation.

We investigated the tumor growth inhibition at molecular level using western blot, high-performance liquid chromatography, immunohistochemistry, gelatin zymography, protein array and real-time PCR techniques.

3.1. The combined liposomal drug therapy inhibited more effectively the growth of B16.F10 melanoma growth than each single liposomal drug therapy.

To measure the effectiveness of the combined liposomal administration of 5 mg/kg SIM and 14 mg/kg DMXAA in comparison with liposomal monotherapy of either 5 mg/kg SIM or 14 mg/kg DMXAA, drugs were injected intravenously on days 11 and 14 after tumor cell inoculation. The therapeutic agents were also administered as free forms in the same doses and according to the same schedule. Effects of free and liposome-encapsulated drugs on tumor growth were evaluated by measuring the tumor volume at day of sacrification (**Figure 11 A, C, E**) and the area under the tumor growth curve (AUTC) (**Figure 11 B, D, and F**).

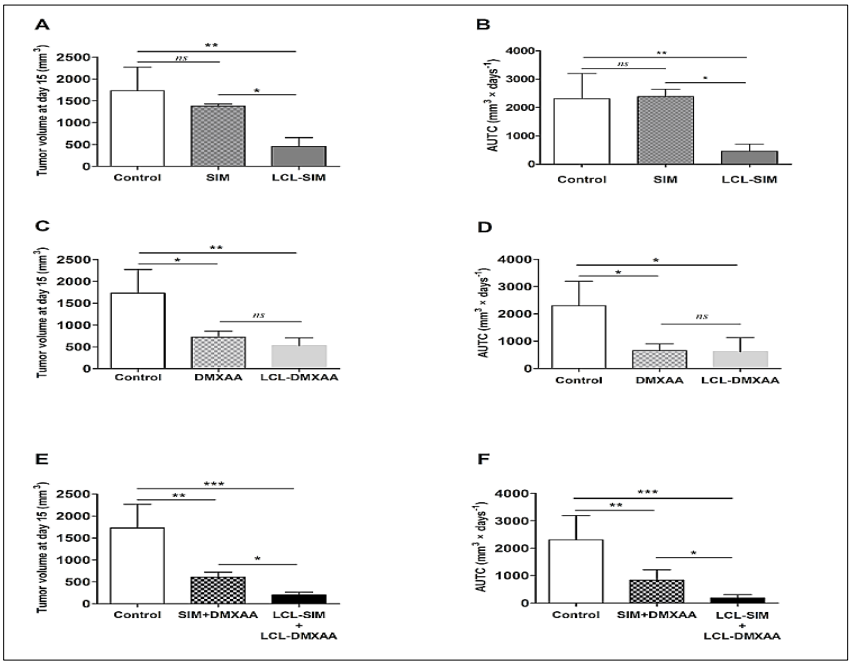

Figure 11: Effects of the combined administration of free and liposome-encapsulated SIM and DMXAA on the growth of *s.c.* B16.F10 murine melanoma. Mice received two *i.v.* injections of therapeutic agents at day 11 and day 14, after cancer cell inoculation Tumor volumes after different treatments at day 15 (when mice were killed) were presented in panels (**A**), (**C**), and (**E**). AUTCs after various treatments were presented in panels (**B**), (**D**) and (**F**). Control – LCL-treated group; SIM – experimental group treated with 5 mg/kg free SIM; LCL-SIM –

experimental group treated with 5 mg/kg SIM as liposome-encapsulated form; DMXAA – experimental group treated with 14 mg/kg free DMXAA; LCL-DMXAA – experimental group treated with 14 mg/kg DMXAA as liposome-encapsulated form; SIM+DMXAA – experimental group treated with 5 mg/kg free SIM and 14 mg/kg free DMXAA; LCL-SIM + LCL-DMXAA – experimental group treated with 5 mg/kg SIM and 14 mg/kg DMXAA as liposome-encapsulated forms. Results were compared with control groups and expressed as mean ± SD of tumor volumes of 6 mice. One way ANOVA test with Bonferroni correction for multiple comparisons was performed to analyze the differences between the effects of the treatments on tumor growth (*ns*, $P>0.05$; *, $P<0.05$; **, $P<0.01$; ***, $P<0.001$).

3.2. Modulatory effects of of liposome-encapsulated agents SIM and DMXAA on B16.F10 murine melanoma oxidative stress.

To link the anti-angiogenic properties of the liposomal therapy with any potential changes in oxidative stress parameters, the levels of specific markers of tumor oxidative stress (MDA, Catalase, and TAC) were determined in tumor tissue lysates (**Figure 12**).

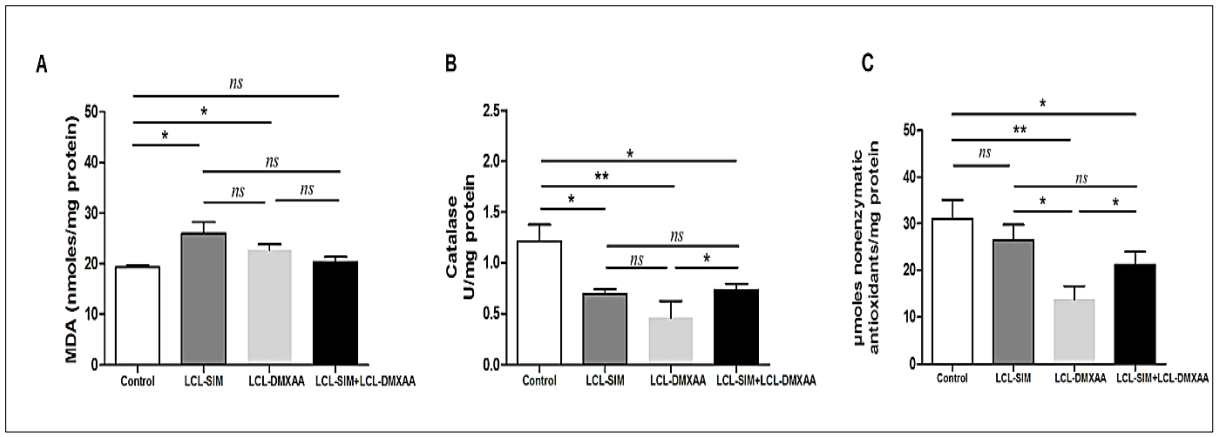

Figure 12: Effects of different SIM and DMXAA liposomal treatments on tumor oxidative stress parameters. **(A)** MDA concentration expressed as nmoles MDA/mg protein; **(B)** Catalase activity expressed as U/mg protein; **(C)** TAC expressed as µmoles nonenzymatic antioxidants/mg protein. All parameters were measured in tumor lysates from mice treated with LCL-SIM and LCL-DMXAA as single or combined therapy. Data represent the mean ± SD of duplicate and triplicate measurements (*ns*, $P>0.05$; *, $P<0.05$; **, $P<0.01$). Control – LCL-treated group; LCL-SIM – experimental group treated with 5 mg/kg SIM as liposome-encapsulated form; LCL-DMXAA – experimental group treated with 14 mg/kg DMXAA as liposome-encapsulated form; LCL-SIM + LCL-DMXAA – experimental group treated with 5 mg/kg SIM and 14 mg/kg DMXAA as liposome-encapsulated forms.

Our data suggested that both single liposomal therapies induced a weak pro-oxidative state represented by increased MDA levels ($P<0.05$, **Figure 12 A**) whereas the combination therapy did not affect MDA levels ($P>0.05$, **Figure 12 A**). In addition, a proportional decrease in enzymatic (catalase) and non-enzymatic (TAC) oxidative stress defence systems was noticed in tumor lysates from groups treated with LCL-SIM ($P<0.05$), LCL-DMXAA ($P<0.01$) and the

combination therapy (P<0.05) (**Figure 12 B, C**), which indicated the lack of an adaptive tumor cell response to drug induced pro-oxidant state.

3.3. Inhibitory effects of the combined liposomal drug therapy on melanoma invasion and metastasis promoters

Evidence of accentuated invasiveness of tumor cells following evasive resistance to VEGF pathway inhibitors (Bergers and Hanahan, 2008), determined us to further look into the effect of our treatments on several established melanoma invasion and metastasis promoters (**Figure 13**).

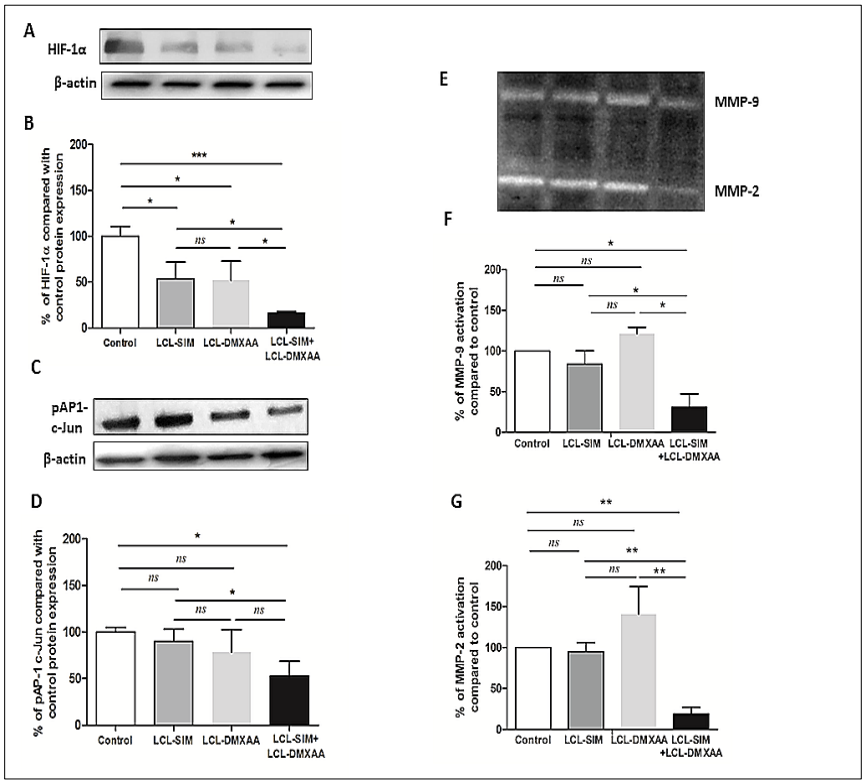

Figure 13: Effects of liposome-encapsulated SIM and DMXAA on intratumoral levels of key invasion and metastasis promoters. (A), **(C)** Western blot analysis showing the effects of different treatments on the intratumor levels of HIF-1α and pAP-1 c-Jun, respectively. β-actin was used as loading control. **(B)**, **(D)** Protein levels of HIF-1α and pAP-1 c-Jun in lysates from treated groups expressed as percentage of control – LCL-treated group. Data represent the mean ± SD of two independent measurements. One way ANOVA test with Bonferroni correction for multiple comparisons was performed to analyze the differences between the effects of the treatments on the proteins involved in the induction of apoptosis (*ns*, P>0.05; *, P<0.05; ***, P<0.001). **(E)**, **(F)**, **(G)** – The effects of different treatments on the activity of microenvironmental matrix metalloproteinases. **(E)** Gelatin zymography analysis of tumor lysates from mice treated with various liposome-encapsulated SIM and DMXAA therapies. Coomassie blue staining highlights gelatinolytic activity corresponding to the active forms of MMP-9 and MMP-2**. (F)**, **(G)** Percentage of MMP-9 and MMP-2 activity in tumor lysates from mice treated with single and combined SIM and

DMXAA liposomal therapies compared to control. Data represent the mean ± SD of two independent measurements. One way ANOVA test with Dunnett correction was performed to analyze the differences between the effects of various treatments on MMP-9 and MMP-2 levels compared to control untreated group (*ns*, $P>0.05$; *, $P<0.05$; **, $P<0.01$). Control – LCL-treated group; LCL-SIM – experimental group treated with 5 mg/kg SIM as liposome-encapsulated form; LCL-DMXAA – experimental group treated with 14 mg/kg DMXAA as liposome-encapsulated form; LCL-SIM + LCL-DMXAA – experimental group treated with 5 mg/kg SIM and 14 mg/kg DMXAA as liposome-encapsulated forms.

3.4. Modulatory effects of single and combined therapies on the expression levels of key arginine metabolic enzymes iNOS and Arg-1

Our results indicated that LCL-SIM+LCL-DMXAA induced the strongest reduction of iNOS (**Figure 14 A**, $P<0.01$) and ARG-1 (**Figure 14 B**, $P<0.001$) expression levels.

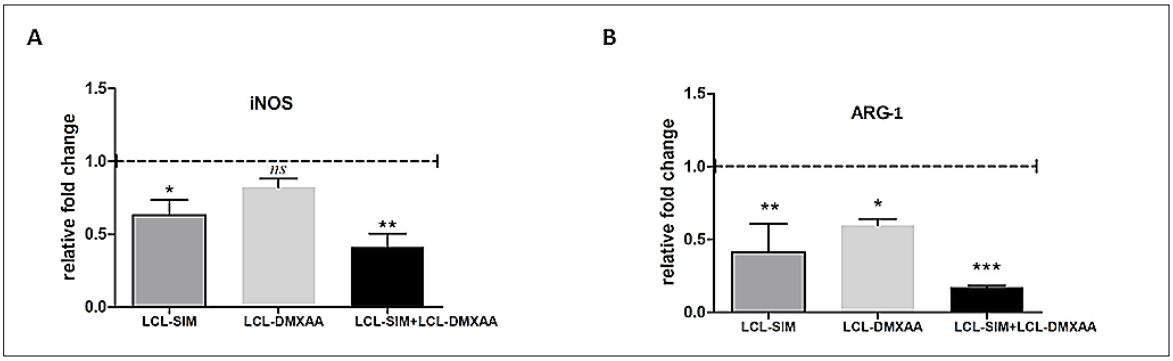

Figure 14: Effects of LCL-SIM and LCL-DMXAA single and combined treatment on TME arginine metabolism *via* arginase and nitric oxide synthase. **(A)**, **(B)** Effects of liposomal SIM and DMXAA administration on the expression levels of iNOS and ARG-1. mRNA was quantified by RT-qPCR and the results are expressed as fold change based on the Ct calculations. Control – LCL-treated group was used as calibrator. Results were expressed as mean ± SD of three independent measurements. Control – LCL-treated group; LCL-SIM – experimental group treated with 5 mg/kg SIM as liposome-encapsulated form; LCL-DMXAA – experimental group treated with 14 mg/kg DMXAA as liposome-encapsulated form; LCL-SIM + LCL-DMXAA – experimental group treated with 5 mg/kg SIM and 14 mg/kg DMXAA as liposome-encapsulated forms. (*ns*, $P>0.05$; *, $P<0.05$; **, $P<0.01$; ***, $P<0.001$).

Chapter VI: Conclusions

The results of the **first study** indicated that the differences in biological activity of the *Ajuga* sp. extracts under investigation were consistent with the differences in polyphenolic compound patterns of each species, confirming that flavonoid combinations can elicit synergistic anticancer effects. Moreover, strong anti-inflammatory actions and a dose dependent "double-edged sword" effect of *Ajuga* sp. extracts on the oxidative stress parameters in B16.F10 murine melanoma cells were observed.

The **second study** reported synergistic antiproliferative effects of the combined treatment consisting of SIM and DMXAA, which promoted an increase in melanin production, leading to an antioxidant shift in the co-culture microenvironment - the principal cause for simultaneous suppression of transcription factors and proteins involved in tumor progression and angiogenesis.

The **third study** reported strong anti-angiogenic and pro-apoptotic effects, as well as a reduction in both enzymatic and non-enzymatic antioxidant capacity of the tumor microenvironment, suggesting that this novel therapeutic combination consisting of LCL-SIM and LCL-DMXAA might be able to influence tumor cell vulnerability to the pro-oxidant pressure elicited before and during metastatic dissemination

Selected references

Akbarzadeh, A., Rezaei-Sadabady, R., Davaran, S., Joo, S.W., Zarghami, N., Hanifehpour, Y., et al. (2013). Liposome: classification, preparation, and applications. *Nanoscale Res Lett* 8(1)**,** 102. doi: 10.1186/1556-276x-8-102.

Alupei, M.C., Licarete, E., Patras, L., and Banciu, M. (2015). Liposomal simvastatin inhibits tumor growth via targeting tumor-associated macrophages-mediated oxidative stress. *Cancer Lett* 356(2 Pt B)**,** 946-952. doi: 10.1016/j.canlet.2014.11.010.

Baguley, B.C. (2003). Antivascular therapy of cancer: DMXAA. *Lancet Oncol* 4(3)**,** 141-148. doi: 10.1016/s1470-2045(03)01018-0.

Balkwill, F.R., Capasso, M., and Hagemann, T. (2012). The tumor microenvironment at a glance. *J Cell Sci* 125(Pt 23)**,** 5591-5596. doi: 10.1242/jcs.116392.

Banciu, M., Metselaar, J.M., Schiffelers, R.M., and Storm, G. (2008). Antitumor Activity of Liposomal Prednisolone Phosphate Depends on the Presence of Functional Tumor-Associated Macrophages in Tumor Tissue. *Neoplasia* 10(2)**,** 108-117.

Casanovas, O. (2012). Cancer: Limitations of therapies exposed. *Nature* 484(7392)**,** 44-46. doi: 10.1038/484044a.

Casian, T., and Iurian, S. (2017). QbD for pediatric oral lyophilisates development: risk assessment followed by screening and optimization. 43(12)**,** 1932-1944. doi: 10.1080/03639045.2017.1350702.

Chen, X., Song, M., and Zhang, B. (2016). Reactive Oxygen Species Regulate T Cell Immune Response in the Tumor Microenvironment. 2016**,** 1580967. doi: 10.1155/2016/1580967.

Csepregi, K., Neugart, S., Schreiner, M., and Hideg, E. (2016). Comparative Evaluation of Total Antioxidant Capacities of Plant Polyphenols. *Molecules* 21(2). doi: 10.3390/molecules21020208.

Denat, L., Kadekaro, A., Marrot, L., Leachman, S., and Abdel-Malek, Z. (2014). Melanocytes as Instigators and Victims of Oxidative Stress. *J Invest Dermatol* 134(6)**,** 1512-1518. doi: 10.1038/jid.2014.65.

Dianzani, C., Zara, G.P., Maina, G., Pettazzoni, P., Pizzimenti, S., Rossi, F., et al. (2014). Drug delivery nanoparticles in skin cancers. *Biomed Res Int* 2014**,** 895986. doi: 10.1155/2014/895986.

Downey, C.M., Aghaei, M., Schwendener, R.A., and Jirik, F.R. (2014). DMXAA causes tumor site-specific vascular disruption in murine non-small cell lung cancer, and like the endogenous non-canonical cyclic dinucleotide STING agonist, 2'3'-cGAMP, induces M2 macrophage repolarization. *PLoS One* 9(6)**,** e99988. doi: 10.1371/journal.pone.0099988.

Egeblad, M., Nakasone, E.S., and Werb, Z. (2010). Tumors as organs: complex tissues that interface with the entire organism. *Dev Cell* 18(6)**,** 884-901. doi: 10.1016/j.devcel.2010.05.012.

Erel, O. (2004). A novel automated direct measurement method for total antioxidant capacity using a new generation, more stable ABTS radical cation. *Clin Biochem* 37(4)**,** 277-285. doi: 10.1016/j.clinbiochem.2003.11.015.

Falleni, M., Savi, F., Tosi, D., Agape, E., Cerri, A., Moneghini, L., et al. (2017). M1 and M2 macrophages' clinicopathological significance in cutaneous melanoma. *Melanoma Res* 27(3)**,** 200-210. doi: 10.1097/cmr.0000000000000352.

Glasauer, A., and Chandel, N.S. (2014). Targeting antioxidants for cancer therapy. *Biochem Pharmacol* 92(1)**,** 90-101. doi: 10.1016/j.bcp.2014.07.017.

Gupta, S.C., Sundaram, C., Reuter, S., and Aggarwal, B.B. (2010). Inhibiting NF-κB Activation by Small Molecules As a Therapeutic Strategy. *Biochim Biophys Acta* 1799(10-12)**,** 775-787. doi: 10.1016/j.bbagrm.2010.05.004.

Hanahan, D., and Weinberg, R.A. (2011). Hallmarks of cancer: the next generation. *Cell* 144(5)**,** 646-674. doi: 10.1016/j.cell.2011.02.013.

Hettinger, J., Richards, D.M., Hansson, J., Barra, M.M., Joschko, A.C., Krijgsveld, J., et al. (2013). Origin of monocytes and macrophages in a committed progenitor. *Nat Immunol* 14(8)**,** 821-830. doi: 10.1038/ni.2638.

Israili, Z.H., and Lyoussi, B. (2009). Ethnopharmacology of the plants of genus Ajuga. *Pak J Pharm Sci* 22(4)**,** 425-462.

Itakura, E., Huang, R.R., Wen, D.R., Paul, E., Wunsch, P.H., and Cochran, A.J. (2011). IL-10 expression by primary tumor cells correlates with melanoma progression from radial to vertical growth phase and development of metastatic competence. *Mod Pathol* 24(6)**,** 801-809. doi: 10.1038/modpathol.2011.5.

Jassar, A.S., Suzuki, E., Kapoor, V., Sun, J., Silverberg, M.B., Cheung, L., et al. (2005). Activation of tumor-associated macrophages by the vascular disrupting agent 5,6-dimethylxanthenone-4-acetic acid induces an effective CD8+ T-cell-mediated antitumor immune response in murine models of lung cancer and mesothelioma.

Kessler, M., Ubeaud, G., and Jung, L. (2003). Anti- and pro-oxidant activity of rutin and quercetin derivatives. *J Pharm Pharmacol* 55(1)**,** 131-142. doi: 10.1211/002235702559.

Liang, C.C., Park, A.Y., and Guan, J.L. (2007). In vitro scratch assay: a convenient and inexpensive method for analysis of cell migration in vitro. *Nat Protoc* 2(2)**,** 329-333. doi: 10.1038/nprot.2007.30.

Liou, G.Y., and Storz, P. (2010). Reactive oxygen species in cancer. *Free Radic Res* 44(5)**,** 479-496. doi: 10.3109/10715761003667554.

Lopez-Bergami, P., Fitchman, B., and Ronai, Z. (2008). Understanding signaling cascades in melanoma. *Photochem Photobiol* 84(2)**,** 289-306. doi: 10.1111/j.1751-1097.2007.00254.x.

Mantovani, A., Allavena, P., Sica, A., and Balkwill, F. (2008). Cancer-related inflammation. *Nature* 454(7203)**,** 436-444. doi: 10.1038/nature07205.

Mills, C.D. (2001). Macrophage arginine metabolism to ornithine/urea or nitric oxide/citrulline: a life or death issue. *Crit Rev Immunol* 21(5)**,** 399-425.

Orsolic, N., Kunstic, M., Kukolj, M., Gracan, R., and Nemrava, J. (2016). Oxidative stress, polarization of macrophages and tumour angiogenesis: Efficacy of caffeic acid. *Chem Biol Interact* 256**,** 111-124. doi: 10.1016/j.cbi.2016.06.027.

Porfire, A., Tomuta, I., Muntean, D., Luca, L., Licarete, E., Alupei, M.C., et al. (2015). Optimizing long-circulating liposomes for delivery of simvastatin to C26 colon carcinoma cells. *J Liposome Res* 25(4)**,** 261-269. doi: 10.3109/08982104.2014.987787.

Redondo, P., Lloret, P., Idoate, M., and Inoges, S. (2005). Expression and serum levels of MMP-2 and MMP-9 during human melanoma progression. *Clin Exp Dermatol* 30(5)**,** 541-545. doi: 10.1111/j.1365-2230.2005.01849.x.

Tasdogan, A., Faubert, B., Ramesh, V., Ubellacker, J.M., Shen, B., Solmonson, A., et al. (2020). Metabolic heterogeneity confers differences in melanoma metastatic potential. *Nature* 577(7788)**,** 115-120. doi: 10.1038/s41586-019-1847-2.